

Article

Different Behaviors of Friction in Open and Closed Forging Test Utilizing Palm Oil-Based Lubricants

Aiman Yahaya *, Syahrullail Samion *, Ummikalsom Abidin and Mohd Kameil Abdul Hamid

Faculty of Mechanical Engineering, Universiti Teknologi Malaysia, Skudai 81310, Johor, Malaysia

* Correspondence: wmainan9@gmail.com (A.Y.); syahruls@mail.fkm.utm.my (S.S.)

Abstract: Increasing demand for manufactured goods in industries such as automobiles, electronics, construction, and aerospace has motivated researchers to develop sustainable manufacturing processes. Most metal-forming lubricants are not eco-friendly; they may cause substantial chemical emissions and constitute a community threat. Bio-oil lubricants are seen as possible replacements for mineral oil-based lubricants. Computational modelling of the forging process uses the finite element method to accelerate and improve design. This research intends to act as a case study and demonstrate how friction behaves differently in open-closed forging tests of different palm oil derivatives. The relationship between the different types of friction was studied using a cold forging test in conjunction with the development of a Coulomb–Tresca friction model. From the results, it can be shown that the friction behavior for the closed forging test (CFT) and the ring compression test (RCT) differs; the CFT exhibits a diversified friction adaptation, while the RCT exhibits a single friction adaptation. From both tests, palm stearin (PS) shows the lowest friction behavior where at RCT the friction is estimated at $m = 0.10/\mu = 0.05$ and the CFT has a varied friction and the average friction is estimated at $m = 0.352/\mu = 0.1626$. On the other hand, commercial metal-forming oil (CMFO) shows the highest lubrication sample in friction, where the value of friction is similar to the no lubricant sample (NA-O), which is ($m = 0.45/\mu = 0.1875$) on the RCT test and ($m = 0.424/\mu = 0.1681$) on the CFT test.

Keywords: open-closed forging; renewable material; Coulomb–Tresca friction; simulation; palm oil



Citation: Yahaya, A.; Samion, S.; Abidin, U.; Abdul Hamid, M.K. Different Behaviors of Friction in Open and Closed Forging Test Utilizing Palm Oil-Based Lubricants. *Lubricants* **2023**, *11*, 114. <https://doi.org/10.3390/lubricants11030114>

Received: 8 February 2023
Revised: 25 February 2023
Accepted: 27 February 2023
Published: 6 March 2023



Copyright: © 2023 by the authors. Licensee MDPI, Basel, Switzerland. This article is an open access article distributed under the terms and conditions of the Creative Commons Attribution (CC BY) license (<https://creativecommons.org/licenses/by/4.0/>).

1. Introduction

The use of mineral-based lubricating oil raises environmental concerns since it is known to have a high degree of toxicity and is seldom spontaneously dissolved in the environment [1]. For many manufacturing procedures, particularly those that create cold work, it is important that the die surface be lubricated. Metal-forming lubricants are used in several processes to improve tool life, metal flow, and energy efficiency by reducing friction and wear at the existing equipment contact [2]. Most commercial lubricants are based on mineral oils, which are not environmentally friendly due to their toxicity and non-biodegradability [3]. Commercial metal-forming oil also involve in open-loop system where the lubricant will end up to the surrounding.

Palm oil is one of the world's most widely used vegetable oils. It is most typically used as cooking oil, also known as palm olein. Due to its greater hydrocarbon chain length and low unsaturation, palm oil may be used as an industrial lubricant [4,5]. The length of the fatty acid chain as well as the amount of unsaturation fatty acid impact the viscosity of palm oil. Many studies have been undertaken to increase the capabilities of palm oil, but the majority of the studies has been restricted to the oil generated up to a single fractionation procedure, such as palm olein and palm stearin (PS) [5]. Many other varieties of palm oil are generated at a greater level of fractionation, such as palm mid olein (PMO). The tribological performance data for these oils is, indeed, quite limited [6].

Open die forging normally entails inserting a solid cylindrical workpiece between two flat dies and compressing it to reduce its height [7]. This process is commonly referred

to as simple upsetting. In reality, the specimen takes on the form of a barrel. In most cases, barreling is generated by friction forces at the die-workpiece interfaces, which act to prevent the outward flow of material at these interfaces from occurring. The workpiece acquires the form of the die cavities (impression) as it is being agitated between the closing dies in closed-die forging, where some of the material flows radially outwards and forms flash [8]. A significant level of pressure is applied to the flash as a result of its large length to thickness ratio. As a result of these stresses, radial material flow in the flash gap is met with a lot of resistance due to the high friction caused by the material. The flash plays a crucial impact in the flow of the material in impression die forging due to the strong friction that facilitates the filling of the die cavities [9].

According to Hafis et al. [10], friction plays a significant role in the generation of stress during metal-forming. Studies have been conducted to determine the impact friction has on forming pressures and the consistency of deformed workpieces. It was suggested by Groche et al. [11] that a friction coefficient might be estimated using data from the normal metal flow that happens throughout a deformation process. There is a critical need for research into friction and its impact on tribology and open-closed forging test. Zhang et al. [12]'s friction model is often regarded via the lens of the traditional friction conceptions whenever (1) and (2):

$$\tau = \mu p \quad (1)$$

$$\tau = mK \quad (2)$$

where,

p = normal pressure

K = shear yield stress

τ = frictional shear stress

μ = Coulomb friction coefficient

m = Tresca shear friction.

The majority of the earlier studies employed minerals and oils that are not suitable for human consumption in the metal-forming process. These oils and minerals include molybdenum disulfide, soap, grease, wax, rapeseed, and many more. It was found that most of this oil showed comparable results with commercial mineral-based oil [2,4,5]. Some of the lubricant has also been modified by the addition of additives, such as those investigated by Du et al., to make it meet the requirements set for commercial lubricants. [13]. It has been shown by Okokpujie et al. [8] that including nanoparticles into copra vegetable oil improves its rheological characteristics and results in less cutting force required during milling.

However, there is a limitation of study on the use of palm oil-based lubricant in metal-forming applications, where the majority of the research applications on palm oil-based were focusing mainly on experimental analysis only [6,14]. A variety of palm oil derivatives were explored and simulated using the finite element method (FEM) to assess as metal-forming lubricant potential. This was done to ensure that the researchers could observe the frictional behavior of each sample test. This study aims to fill a research gap by comparing friction behavior under various types of forging processes using the best palm oil derivatives based on their physicochemical properties by modelling finite element method of sample lubricant with different applications of the forging process (Open and closed forging).

2. Methodology

2.1. Physicochemical Properties of Sample Lubricants

Table 1 summarizes the physical parameters of all six kinds of palm oil-based lubricants. The six types of palm oil include refined, bleached and deodorized palm oil (PO), palm fatty acid distillate (PFAD), palm olein (PL), palm stearin (PS), palm kernel oil (PKO), and palm mid-olein (PMO).

Table 1. Physical properties of palm oil [15].

Lubricant	PKO	PO	PS	PL	PMO	PFAD	CMFO	Test Method
Density (kg/m ³) @ 25 °C D1298-85(90)	0.887	0.880	0.870	0.890	0.895	0.873	0.900	ASTM
Kinematic Viscosity (mm ² /s) @ 25 °C	45.77	215.47	48.29	46.74	54.6	120.14	146.24	ASTM D445-94
Kinematic Viscosity (mm ² /s) @ 40 °C	35.36	189.40	38.01	35.00	50.6	96.35	107.71	ASTM D445-94
Kinematic Viscosity (mm ² /s) @ 100 °C	11.24	18.20	8.56	14.4	13.2	8.9	11.2	ASTM D445-94
Viscosity index, (VI)	329	106.00	213	426	272	48	88	ASTM D2270
Pour point (°C)	21.0	34.0	37.3	9.0	15.0	35	−24.0	ASTM D9793
Melting point (°C)	27.5	48.50	44.0	21.5	18.50	38.0	-	-
Flash Point (°C)	205	205	315	318	324	135	236	-
Cloud Point (°C)	-	-	-	9.5	18.5	-	-	-
Iodine value (WIJS)	17.8	17.8	27.8	56.15	48.23	24.80	-	-
Free fatty acid (%)	0.06	0.06	0.05	0.07	0.15	86.4	-	ASTM D664
Peroxide value (PV)	0.84	0.85	1.04	0.95	0.92	1.58	-	-

One measure of a fluid's resistance to movement through its environment is its viscosity. Utilizing oil with a higher viscosity resulted in a thicker oil coating; however, this increased flow resistance and reduced the ability to protect the contact surface [6,15]. It is possible that low-viscosity oils may help in the boundary lubrication regime, but in the sliding system, they'll be rapidly worn away by the contact surfaces. Lubricant oil with a high viscosity index (VI) is generally considered as a good lubricant [14,15]. Higher VI meant that the viscosity of the oil did not vary much when the temperature is raised. That is, the oil's viscosity profile suffered fewer phase shifts, resulting in greater heat stability. In terms of viscosity index, PKO had the greatest value of 329 and commercial metal-forming oil had the lowest value of 88. The slip melting point is another essential characteristic that indicates lubricant oil fluidity. In the palm oil sector, the slip melting point was the temperature at which all crystal nuclei were melted, which occurred most often in the stearin fraction. The degree of unsaturation of fatty acid molecules is determined by the iodine value (IV) [16]. It is an essential parameter since it reveals the fats and oils' properties. IV is highly correlated with the cloud point and the fatty acid makeup of the oil.

The top three varieties of palm oil-based lubricant were chosen using the scoring system shown in Table 2. The score is determined by the following rank (1 is good to 6 is poor) and is based on the reasoning provided in Table 1. The oil with the lowest score was rated first, followed by the others.

Table 2. Evaluation score of palms oil-based lubricant.

Lubricant	PKO	PO	PL	PS	PMO	PFAD
Density (kg/m ³) @ 25 °C	3	4	5	1	6	2
Viscosity index, (VI)	2	5	1	4	3	6
Pour point (°C)	3	6	5	1	4	2
Melting point (°C)	2	5	6	1	3	4
Flash Point (°C)	5	4	3	2	1	6
Iodine value (WIJS)	6	2	1	4	3	5
Free fatty acid	1	4	6	2	3	5
Peroxide value	1	2	4	5	3	6
Total score	23	32	31	20	26	36

According to Table 2, PS leads the pack with a total score of 20 and is followed by PKO at 23. The cloud point feature was not taken into account in this score assessment since it cannot be identified in certain oils. It may be concluded that PS, PKO, and PMO

have shown acceptable basic lubricant oil characteristics and have been chosen as a palm oil-based lubricant in the metal-forming processes.

Gas-liquid chromatography (GLC) was used to determine the chemical characteristics in terms of fatty acid composition (FAC) as shown in Table 3. The sample was separated into its constituents depending on their affinity for the liquid and mobile phases [16]. According to Table 3, PKO has the largest amount of saturated fatty acid, coming in at 82.3%, while PMO has the least amount, falling in at 53.5%. PS and PMO have a pattern that is comparable, in that they have a high concentration of palmitic and oleic acid, in contrast to PKO, which has a high concentration of lauric acid. This can be seen by looking at each composition of the fatty acid. Figure 1 shows the experimental set-up for both testing (open and closed forging).

Table 3. Composition of fatty acids in palm oil used as a lubricant [2].

FAC (% by Gas Chromatography)	PS	PKO	PMO
Caprylic acid C8:0	-	3.6	-
Capric acid C10:0	-	3.5	-
Lauric acid C12:0	0.16	47.8	0.5
Myristic acid C14:0	1.16	16.3	1.1
Palmitic acid C16:0	54.31	8.5	45.0
Stearic acid C18:0	4.71	2.6	6.4
Oleic acid C18:1	32.31	15.3	37.3
Linoleic acid C18:2	6.68	2.4	8.8
Linolenic acid C18:3	0.3	-	0.2
Arachidic acid C20:0	0.37	-	0.5
Eicosenoic acid C20:1	-	-	0.1
Saturated fatty acid	60.71	82.3	53.5
Mono-unsaturated fatty acid	32.31	15.3	37.4
Poly-unsaturated fatty acid	6.98	2.4	9
IV	33	17.8	54

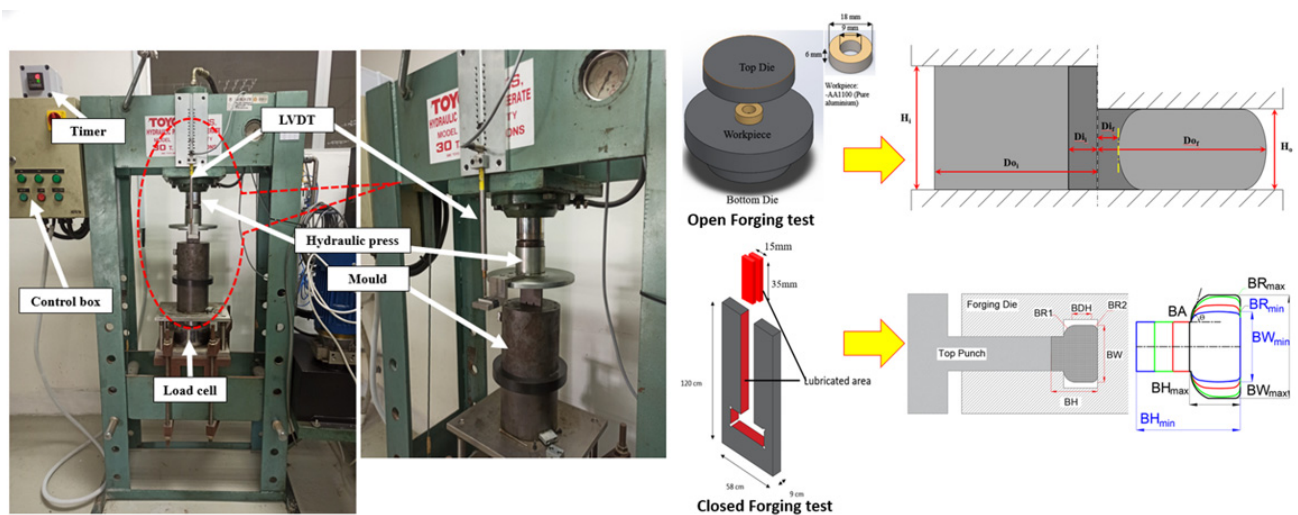


Figure 1. The open-closed forging test set up [15,17].

2.2. Metal-Forming Test

In order to evaluate the frictional behavior with various derivatives of palm oil-based lubricants, two main tests were conducted, which were open forging and closed forging test. A hydraulic press machine, similar to the one seen in Figure 1, was used to conduct an analysis on each and every test sample. The experimental materials and conditions are summarized in Table 4.

Table 4. Materials and conditions for experiments [14,17].

Properties	Open Forging Test	Closed Forging Test
Workpiece	Pure aluminum (A1100)	
Workpiece Hardness (Hv)	Before annealing = 134.8 After annealing = 52.6	
Tooling material	SKD-11	
Workpiece size (mm)	18:9:6	35 × 15 × 4.5
Reduction in height	~10%, ~20%, ~30%, ~40% and ~50%	
Lubricant quantity (mg)	~5 mg	~10 mg
Temp (°C)	24–27 (Room temperature)	
Compression speed (mm/s)	1	

2.3. Finite Element Method

The DEFORM-3D optimization routines employ three types of variables while working toward an optimum design: design variable (independent variable), state variable (dependent variable) and objective function. The height is defined as a design variable with an initial value of 35 mm and the billet width as a function of the billet height. The state variable are quantities that are used to define a constraint for the design and also known as a dependent variable with typical response quantities such as stresses and displacement [18]. Objective function in closed forging die is projected to the complete die filling without defects. The flow of the A1100 in the mold is analyzed throughout this study, and the aim of the simulation is to identify the maximum possible height over which the material may flow. In the DEFORM-3D parametric design language, they are provided as scalar parameters [19]. In an optimization study, the independent variables are defined, such as tool and die geometry, lubricant, friction, and amount of deformation. Variables in the design are represented by their vectors, which are:

$$x = [x_1 \ x_2 \ x_3 \ x_4 \ \dots \ x_n] \quad (3)$$

Each design variable has n associated constraints, or maximum and minimum values;

$$\underline{x}_i \leq x_i \leq \bar{x}_i \quad (i = 1, 2, 3, \dots, n) \quad (4)$$

where:

n = number of design variable.

x_i = Design variable

\underline{x}_i = Lower limit

\bar{x}_i = Upper limit

The limits placed on the design variables are known as side constraints, and they set the bounds that define the so-called viable design space.

Now, minimize

$$f = f(x) \quad (5)$$

Subject to

$$g_i(x) \leq \bar{g}_i \quad (i = 1, 2, 3, \dots, m_1) \quad (6)$$

$$\underline{h}_i \leq h_i(x) \quad (i = 1, 2, 3, \dots, m_2) \quad (7)$$

$$\underline{w}_i \leq w_i(x) \leq \bar{w}_i \quad (i = 1, 2, 3, \dots, m_3) \quad (8)$$

where:

f = objective function

g_i, h_i, w_i = state variables containing the design, where under- and over-bars denote minimum and maximum values (input as max and min on optimization variable commands). m_1, m_2, m_3 are the total number of constraints placed on state variables by their respective ranges of allowable values. Due to their correlation with the vector (x) of design variable, state variables are often called “dependent variables”. The purpose of the constrained minimization problem represented by Equations (3) to (5) is to minimize the objective function $f(x)$, subject to the restrictions given by Equations (6) to (8).

Correlation between real stress–strain data acquired from pure aluminum A1100 workpiece using the Instron 5982 universal testing equipment is used to describe the material. The results of the tensile tests performed on the three samples given for this study are shown in Figure 2. Table 5 shows the parameters that are used in FEA of both openforging test (RCT) and closed forging test (CFT). As suggested by Li et al. [20], the following may be used as a first estimate for the plastic region curve of stress–strain:

Table 5. Parameters used in FEA of forging test.

	FEA Program	Scientific Forming Technologies Corporation (SFTC)	
	Compiler for User Subroutines	DEFORM-3D Ver-10.2	
	Material Plasticity Method	Elastic-Plastic formation	
	Die Material Type	Rigid	
	Punch Velocity	1 mm/s	
ANALYSIS OPTIONS	Number of steps	RCT 50	CFT 400
	Iteration Method	Newton-Raphson	
	Remeshing	Global remeshing, overlay quad type, depends on element distortion,	
	Number of meshing	RCT 55000	CFT 45000
	Deformation	Active in FEM + meshing	
	Temperature	20 °C	
CONTACT	Inter-Object Data Definition	Coulomb-Tresca friction model	
	Relative Sliding Velocity	Default (=0)	
	Tolerance	0.0256	
MATERIAL		Model	
	Young’s Modulus	A1100 = 68.900 GPa	
	Poisson’s Ratio	A1100 = 0.33	

It can be observed in Figure 2 that stress data are only accessible up to a value of $\varepsilon_{true} = 0.032$ in this case. However, for this extension, the smallest size as well as the chord length at the neck are required. Because tensile stress causes metals to lose their formability, upsetting is used to increase the strain values of the metals under test. If the flow curve is simply to be calculated for low stresses, the tensile test will offer sufficient information for this purpose. If the flow curve calculated for low strains can be extended to greater strains, this test is even effective in certain conditions. The stress–strain curve in the plastic region can be approximated by:

$$\sigma = H\varepsilon_p^n \quad (9)$$

$$\varepsilon_p = \left(\frac{\sigma}{H}\right)^{1/n} \quad (10)$$

where

ε_p = plastic strain

H = strength coefficient
 n = unitless pressure hardening exponent

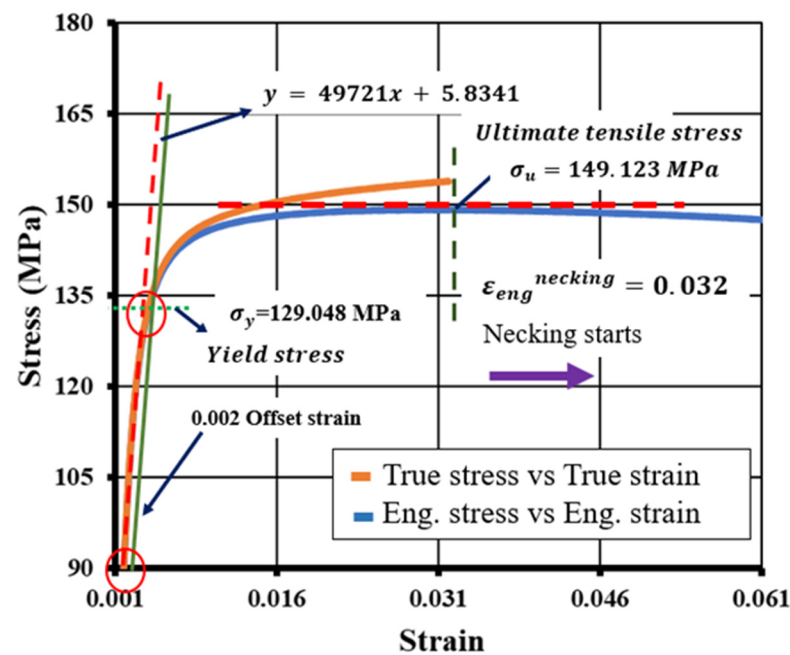


Figure 2. The tensile testing resulted in a stress–strain curve for AA1100 [15].

It was proposed by Ramberg and Osgood that this connection may be utilized to anticipate the shape of the stress–strain curve for any given material. Tensile and yield strengths of this plastic may be determined using the following equations [21];

$$\sigma = 140.82244(\varepsilon)^{0.01405} \quad (11)$$

where

σ = true stress

ε = true strain.

The design of the rig was based on the assumption that all of its components were solid bodies, which was made possible by the use of a stiff surface analysis. The aluminum alloy utilized in this study is one that, as noted by Szala et al. [22], has generally been a strain-hardening and cold-forming material.

3. Results and Discussion

3.1. Open Forging Test

The effects of several palm oil-based lubricants on load variation throughout the forging process were investigated, and the results were compared to those obtained without lubrication (NA-O) and a CMFO lubricant used as a benchmark. A direct relationship between force and die stroke was discovered in experiments, as shown in Figure 3. The graph displays the initial deformation as well as the after deformation, with the early deformation beginning at 0 kN and ending at 3 mm (50%) compression of the die stroke with varying load values for each sample.

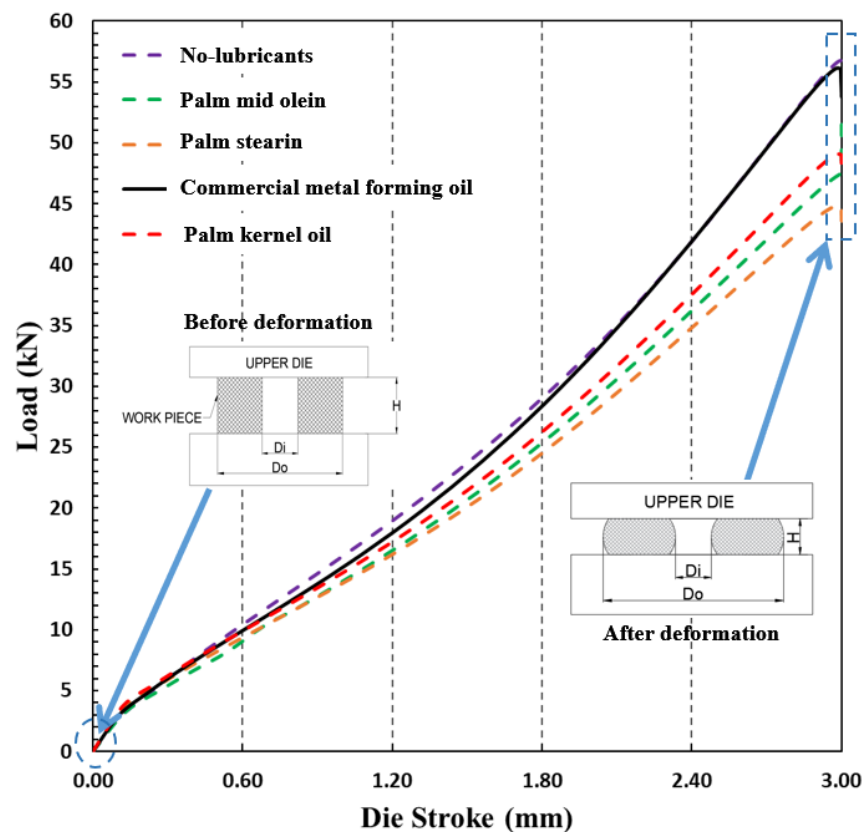


Figure 3. Testing the forging force of a NA-O, PKO, PS, PMO, and CMFO.

From the result obtained, the compression load is directly proportional to the die stroke. The absence of lubrication in the workpiece and the interaction between the metals have both indicated a growing load, and it is clearly evident that the NA-O sample had the largest degree of compression during the whole of the test where the max load is around 56.71 kN. According to Tiong et al. [23], the presence of lubricant normally contributes to the reduction of friction, which consumes less compression load; however, the presence of CMFO in ring comparison test shows that the load somewhat is comparable to the NA-O sample, where the load is lower only at 10% to 30% die stroke with max compression load of 55.99 kN. Compared to the benchmark lubricant (CMFO), all of the samples of the palm oil-based lubricant show a considerable reduction in compression load, indicating that it has the potential to be used as a lubricant in metal-forming process. PS, on the other hand, demonstrates to be the most desirable lubricant in RCT tests with the max compression load at 44.85 kN, where the compression load exhibited the lowest load when compared to other palm oil-based lubricants. PKO is a well-known palm oil-based lubricant that has been tested as an engine oil lubricant and in some cases, such as the one proposed by Aiman et al. [17], the lubricant performed better than the mineral oil. PMO is also one among the products of palm oil, but it has received less attention from researchers than other palm oil products, particularly in the metal-forming process. This product has shown some intriguing findings, which include a reduced compression load (48.56 kN) in comparison to PKO (49.08 kN) and CMFO sample in RCT test.

A lubricant is acceptable for use on the contact surface during extrusion if it keeps the extrusion load within an acceptable range, as stated by Wang et al. [24]. This is one of the criteria for determining whether or not a lubricant is suitable for this application. In these situations, the reduced compression load of PS, PKO, and PMO might be related to the material's physical behavior, in which it exists in a semi-solid form at ambient temperature and completely liquidizes when heated to 40 °C [25]. As highlighted by Maleque et al. [26], palm oil's high concentration of free fatty acids (FFA) contributes to the creation of a thin lubricating coating between the taper die and the work material. According to the data

shown in Table 3, palm oil seems to include oleic acid, which may aid in reducing the amount of drag encountered by moving objects.

The strength of a fatty acid chain is determined by how the densely packed alkyl chain reacts to the accumulated short range Van der Waals interactions between neighboring methyl groups [27]. A greater affinity on the metal surface was achieved with a higher closed packed density. The ninth and tenth carbons of the fatty acid's chain are double-bonded, making it unsaturated. Confirmed by Campen et al. [28], this double bond causes the unsaturated fatty acid oleic acid to adopt a cis-configuration, making it difficult for the molecules to adopt a linear shape. Unsaturated fatty acids are therefore far less efficient in forming tightly packed monolayer soap films. Less compact packing density causes fatty acid chain molecules to have less attraction for metal surfaces. Meanwhile, the molecules of palmitic and stearic acid, which are saturated fatty acids, have a great capacity to pack tightly and effectively on metal surfaces (Wood et al., 2016). The metal surface was protected by PS (C16:0 = 54.31% and C18:0 = 4.71%) and PMO (C16:0 = 45.0% and C18:0 = 6.4%) with a high amount of saturated fatty acids, which also showed excellent molecular packing and offered a decreased compression load compared to PKO as discussed by Zulhanafi et al. [6].

Calibration Curve and Optimization Process

As a means toward a more complete understanding of frictional behavior, it is crucial to compare the experimental result with the findings of the FEM. In a mathematical optimization problem, the objective function is the real-valued function whose value is to be reduced or maximized relative to the set of feasible solutions. Figure 4 depicts the comparison of exploratory results with the contact calibration curves, which was used to determine the TSF and CFC. For the purpose of identifying optimal interaction parameters, Zhang et al. [29] claim that there is no widely accepted method for matching experimental data with the optimum calibration curve. As previously indicated [13], Equation (12) was utilized as a benchmark to establish the correlation of friction between Tresca shear friction (TSF) and Coulomb friction coefficient (CFC).

$$\frac{|d_{\mu} - d_m|}{d_0} < e \quad (12)$$

where

d_{μ} = inner diameter of the CFC

d_m = inner diameter of the TSF

d_0 = inner diameter before deformation

e = positive smaller of the two inner diameters.

A lower positive value e is obtained by comparing the inner diameters of the specimens. Because of the precision of the finite element model, Zhang et al. [13] noted that the inner diameter of the specimen remains almost constant for $e < 0.005$ despite a little fluctuation in friction. As a result, $e = 0.005$ may be a good figure to use to determine whether the narrowing of the metal ring's inner width agrees with the appropriate calibration curve. Using Equation (12), we can define Equation (13) to evaluate the friction parameters, and we know that $e = 0.005$ or 0.5% is the smallest positive value that best describes the situation.

$$\frac{|D_{Exp} - D_{\mu,m}|}{D_0} = |\delta D_{Exp} - \delta D_{\mu,m}| < e \quad (13)$$

where

D_{Exp} = inner diameter of experimental data

δD_{Exp} = change in inner diameter of experimental data.

$D_{\mu,m}$ = inner diameter of each friction representation

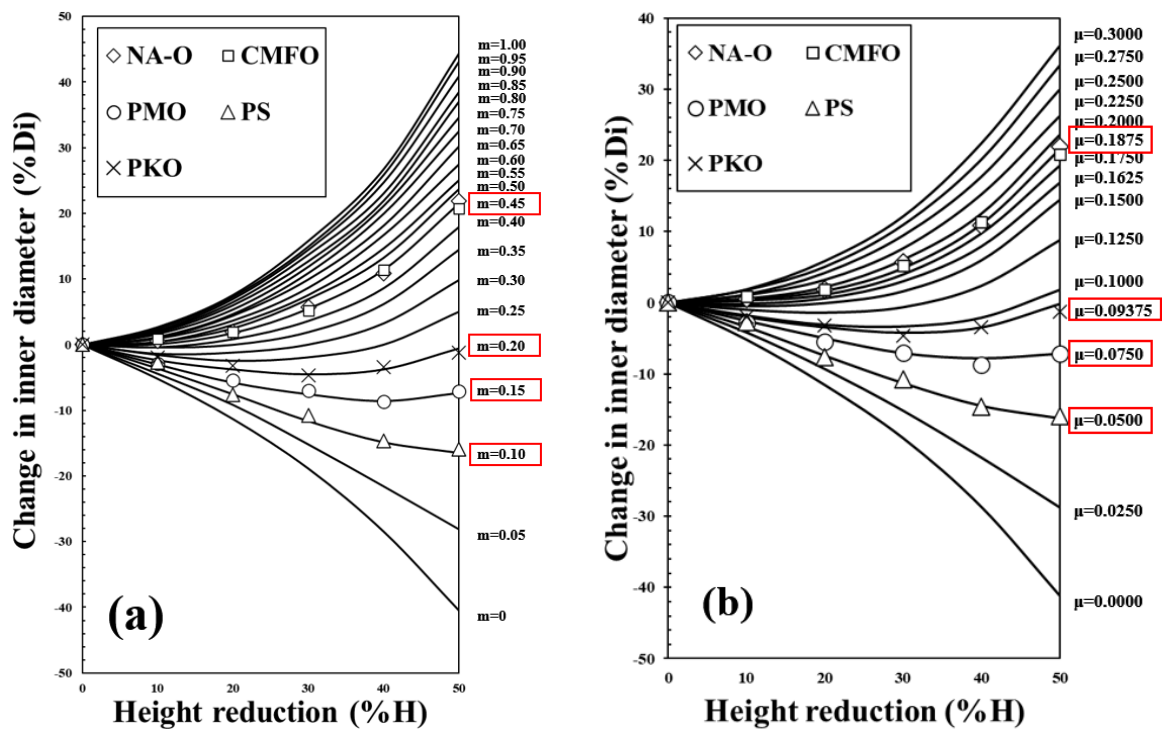


Figure 4. Validation of experimental result of change in inner diameter for each height reduction (a) Tresca shear friction and (b) Coulomb friction coefficient.

The internal diameter changes brought about by a minor shift in μ or m for a moderate reduction in height are negligible. The discrepancies between the test findings and the fitted calibration curves were determined and analyzed using Equation (13).

Figure 4 depicts the calibration curves for each of the samples after the e values were determined for each one and compared to the FEM. The line in this figure represents the simulation data, while the point in the figure is the actual experimental result. The data reveal that the friction is best matched at $m = 0.45$ and $\mu = 0.1875$ for the no lubricant sample (NA-O), indicating that this sample has the maximum frictional value. When compared to the deformation shown in the NA-O sample, the CMFO result shows a similar trend. The PS, on the other hand, had the least amount of friction at $m = 0.1$ and $\mu = 0.05$, as shown by the findings from the sample that was based on palm oil. When compared to the PS, the PMO exhibits a somewhat greater amount of friction where the values for friction are $m = 0.15$ and $\mu = 0.075$. PKO demonstrates the greatest amount of friction in palm oil based on the values of $m = 0.20$ and $\mu = 0.09375$.

Data from the cold work compression test with the lubricant sample are compared with the force applied in the FEM to validate the friction coefficient. The steady-state effects of force owing to displacement were reported in the experimental investigation at a variety of stroke locations and compared with the FEM simulations with varying shear friction factors.

Figures 5 and 6 show the result of comparing the TSF and CFC calibration curves with the validation of compression load results; this shows that all of the sample tests have a strong connection with a single friction behavior. According to the findings (Figure 5a,b), there is a clear connection between the friction of the NA-O sample and the value of $m = 0.45/\mu = 0.1875$, which is the same as the value for the CMFO sample. From Figure 5e, PS showed the lowest friction and has a high connection to the $m = 0.10/\mu = 0.05$, whereas the friction behaves $m = 0.15/\mu = 0.075$ for PMO (Figure 5c). PKO exhibits the lowest amount of friction in comparison to the palm oil-based lubricant, in which the compression load is precisely equivalent to the $m = 0.20/\mu = 0.09375$ expression.

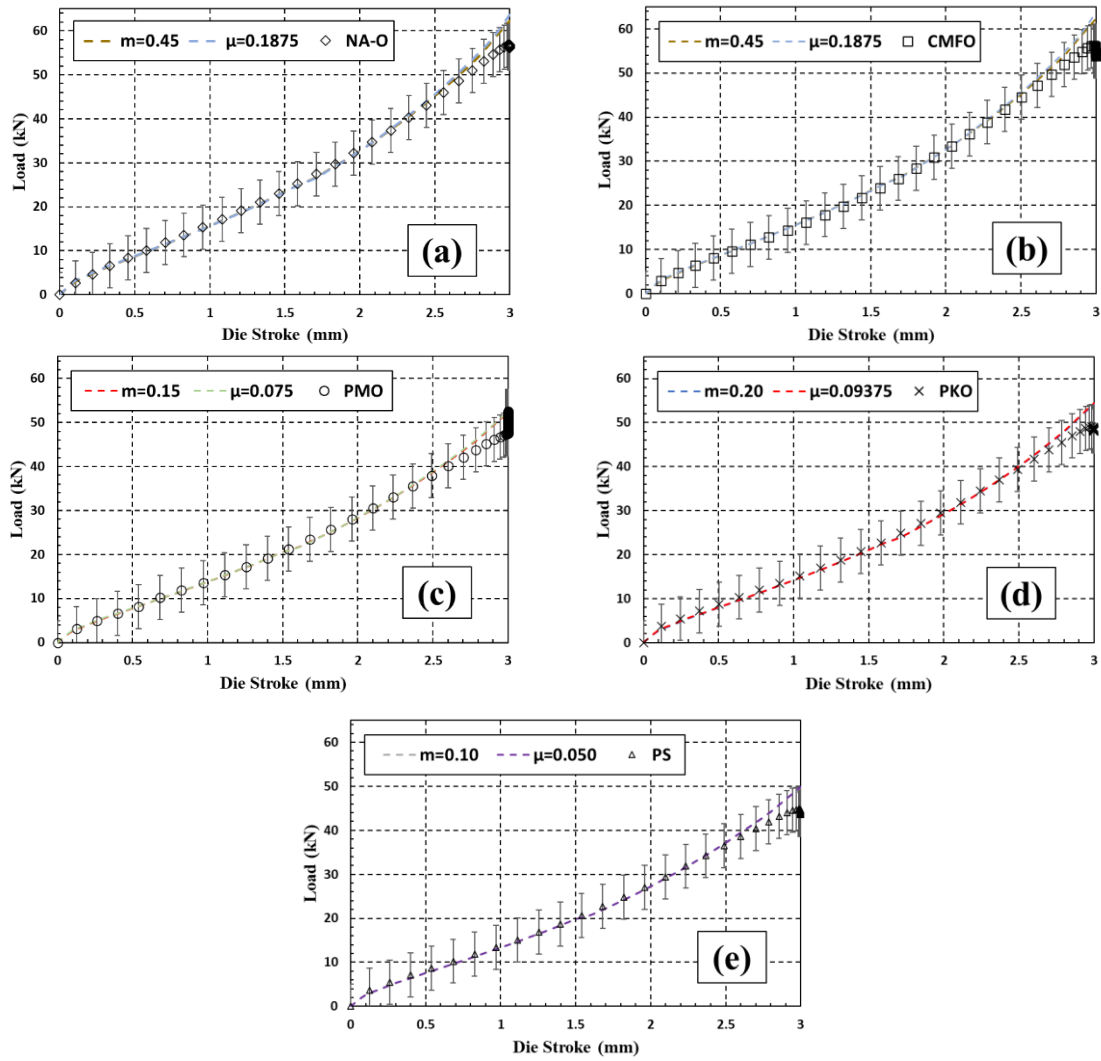


Figure 5. Force against height of deformation: FEM modelling and experimental data for (a) NA-O, (b) CMFO, (c) PMO, (d) PKO, and (e) PS [17].

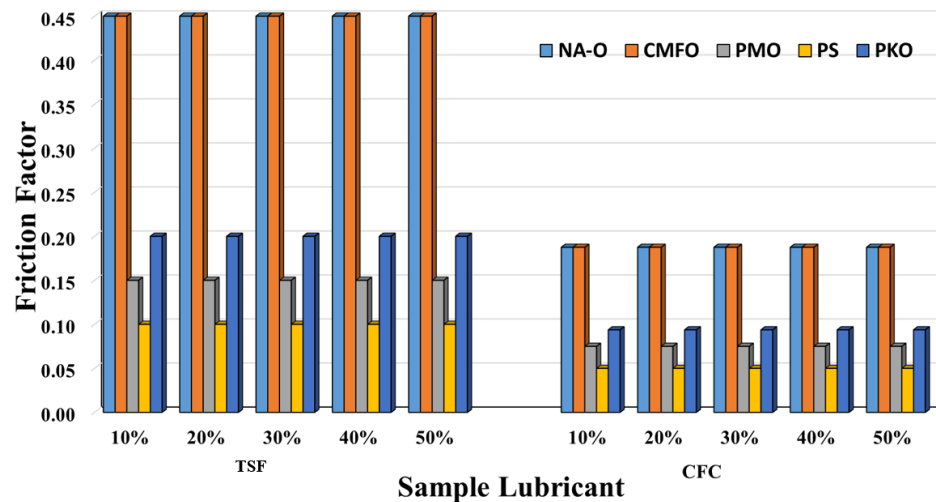


Figure 6. Summary of friction behavior for each component of the sample test following FEM optimization for open forging test.

The data that were collected throughout the process of calibration and optimization may be used to determine the efficiency of each sample. Equation (14) has been used to estimate the effectiveness of the lubricant in terms of the efficiency of friction lubrication percentage ($m = 0, \mu = 0$ as a 100% efficacy that is denoted as $m\mu_0$). This comparison is made in relation to the situation where there is no lubricant present (NA-O) (Zhang et al., 2019). Where $m\mu_{NA-O}$ = friction of non-lubricated sample and $m\mu_{sample}$ is the friction that occurs in each lubricated sample.

$$\left| \frac{(m\mu_{NA-O} - m\mu_0) - (m\mu_{NA-O} - m\mu_{sample})}{(m\mu_{NA-O} - m\mu_0)} \right| \times 100\% = efficiency\% \quad (14)$$

According to the results of the calculation of efficiency provided by the CMFO, there is no improvement where the friction is maintained at the same level as in the NA-O sample. The PS, on the other hand, has the highest efficiency, which decreased the friction by around 77.8%, while the improvement for the PMO was approximately 66.7%. PKO, on the other hand, demonstrates a worse performance in comparison to PS and PMO, which is somewhere about 55.6%.

According to Caminaga et al. [30], a lubricant may be acceptable for usage in the deformation zone during the extrusion phase if the lubricant could lower the extrusion stress to a decent degree. It has been demonstrated that as metal-to-metal contact increases, the mechanism requires more energy to slide the material and raise the compression load due to higher friction. Besides that, NA-O and CMFO shows that the presence of lubricant does not contribute to an improvement in the friction behavior in these areas.

As per Tiong et al. [23], PS is semi-solid at ambient temperature, would entirely liquidate till it crosses 40 °C, and may display sluggish mobility during the forging process where PMO also conduct a similar characteristic. These physical conditions reduce friction and compression force during transformation. The amount of work piece that came into contact with the die throughout the process was small. According to the findings of a previous research, one of the benefits of having a higher viscosity is that it may reduce the amount of damage and wear that is caused to surfaces by retaining the layers that are generated between the rubbing surfaces [31]. The shift from a mixed to a boundary lubrication regime is facilitated by a lower viscosity, which results in the surface being subjected to a greater coefficient of friction and increased wear [16]. This behavior may account for the fact that PKO, as shown in Table 1, has higher friction due to its lower viscosity compared to the other palm oil-based lubricant [31].

Moreover, FFA-penetrating palm oil-based lubricant provides a thin fluid film-lubricating layer between the work material and taper die, as described by Maleque et al. [26]. The oleic acid content of palm oil is shown in Table 2, which may decrease relative motion friction. Since glycerol normally binds to fatty acid to generate the thin film between both the surfaces under rubbing action, higher rates of glycerol and fatty acid contribute through a thicker layer, decreasing friction, wear, and load of extrusion, as stated by Yingying et al. [32]. A longer carbon chain in the FFA composition indicates a higher concentration of FFA, as shown by the aforementioned study, which demonstrates that the PS has potential as a metal-forming lubricant.

3.2. Closed Forging Test

The effects of several types of palm oil-based lubricant, as well as no lubrication and commercial metal-forming lubricant, on the load variation of the forging process were investigated. Figure 7 demonstrates the experimentally established connection between punch load and die stroke. In the first stage, a comparison of the sample lubricants reveals that all of them follow a fairly identical trajectory, in which the load abruptly escalates. A unique pattern emerges in the second phase of the lubricant's influence. By measuring how much friction is reduced during the compression test, researchers can now estimate how well the lubricant sample performs. When compared to alternative lubricants, palm

stearin (PS) has shown superior lubrication efficiency, with the lowest compression load appearing in the third stage and remaining constant all the way through to the final product production. A study by Tiong et al. [23], found that at ambient temperature PS has the consistency of a semi-solid but may become a fluid at temperatures of 40 °C or beyond. This quality may aid lubricants in decreasing the amount of metal-to-metal contact that takes place by decreasing the amount of friction between metallic surfaces. Comparatively, the compression load of CMFO is much higher than that of other palm oil-based lubricants, such as PKO and PMO. The iodine and moisture found in palm oil have been demonstrated to provide anti-friction properties between two moving metal substrates [33]. Reduced friction and compression force during the transitional stage suggest that as little metal as possible was brought into contact with the die and the workpiece.

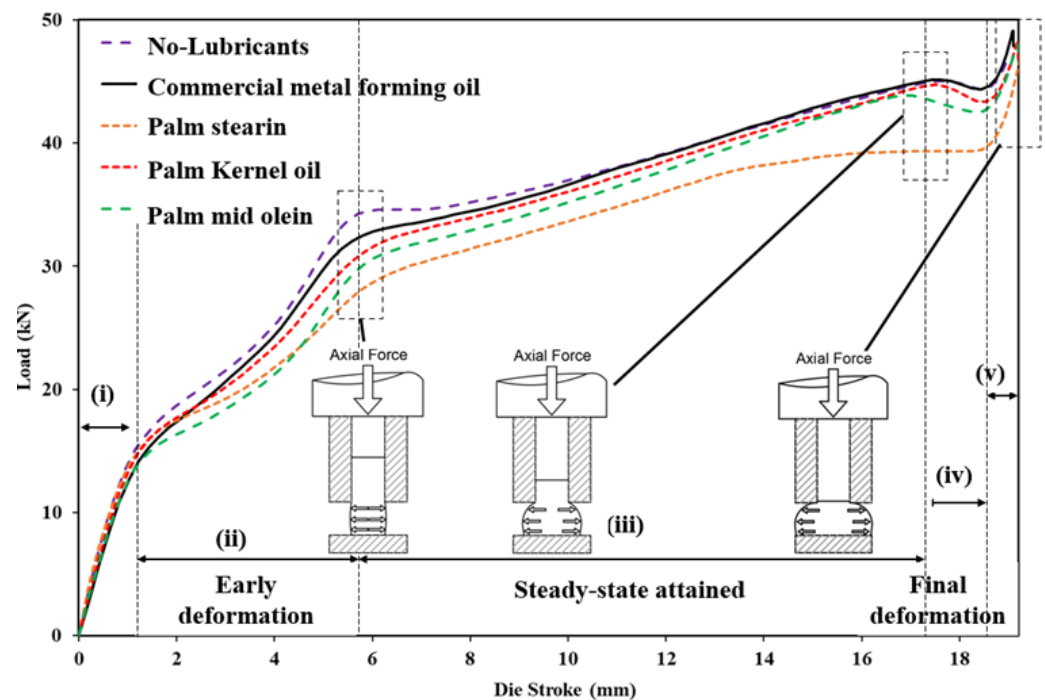


Figure 7. Compression load of NA-O, CMFO, PS, PKO, and PMO at certain die stroke.

Table 1 demonstrates that oleic acid, which is assumed to be present in palm oil, could assist in lowering relative motion blur. Moreover, free fatty acids (FFA) penetrating palm oil aid in forming a thin lubrication coating between the taper die and the workpiece material, as indicated by Maleque et al. [26]. Glycerol normally binds to fatty acid to produce a thin film between the two surfaces when rubbing happens; increased quantities of glycerol and fatty acid contribute through a thicker layer, which lowers friction, wear, and compression stress, as stated by Yingying et al. [32]. The aforementioned analysis reveals that the PS is appropriate since the FFA content has a much longer carbon chain than the PMO and PKO.

3.3. Optimization and Analysis of FEM

The compressed sample's billet width and billet height were measured, along with a few other design factors, so that test results could be compared to those obtained from the simulation. Furthermore, as was previously said, there is no universally accepted method for determining how to best correlate experimental data with the appropriate calibration curve, which is necessary for determining interaction conditions [29]. As stated by Zhang et al., [12] Equations (15)–(17) was utilized as a benchmark in order to assess the form of the relationship that exists between TSF and CFC.

$$\frac{|BW_{exp} - BW_{\mu,m}|}{BW_0} = |\delta BW_{Exp} - \delta d BW_{\mu,m}| < e \quad (15)$$

$$%BW = \frac{BW_o - BW_{exp,m,\mu}}{BW_o} \times 100\% \tag{16}$$

$$%BH = \frac{BH_o - BH_{exp,m,\mu}}{BH_o} \times 100\% \tag{17}$$

where

BW_{exp} = experimental width

$BW_{\mu,m}$ = width for the specimen of TSF or CFC model

BW_0 = width before deformation

e = smaller positive number from the specimen comparison

With the use of Equation (15), the gaps that were found between the results of the experiments and the fitted calibration curves were computed and illustrated in Figure 8. The examination concluded that the experimental results were in close agreement with one calibration curve, with just a few minor discrepancies amounting to less than 0.5% of the total.

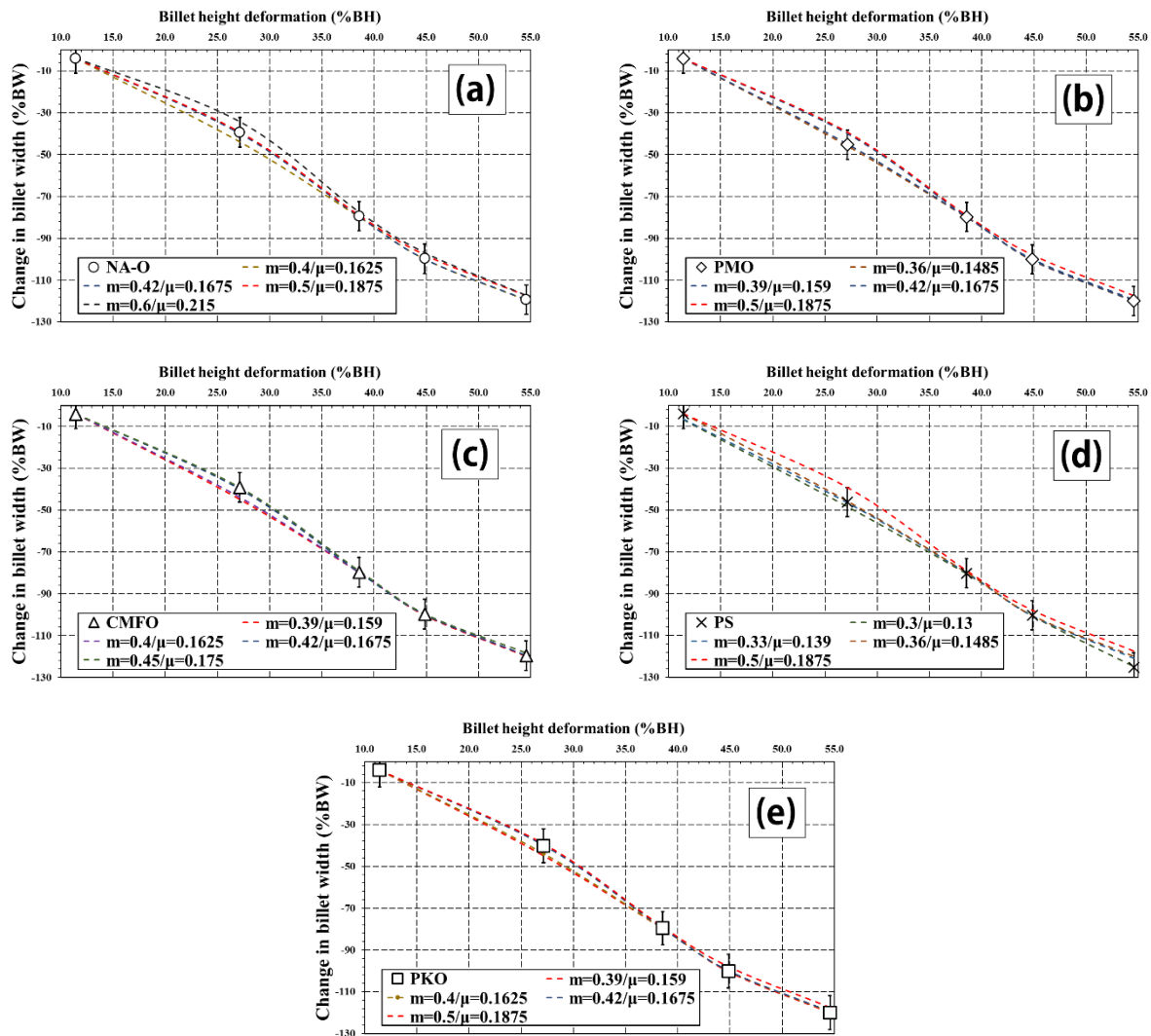


Figure 8. Calibration graph of closed forging test for (a) NA-O, (b) PMO, (c) CMFO, (d) PS, and (e) PKO.

Into a more precise calculation of the lubricant sample’s friction coefficient, the FEM is used to compare the collected data to the applied force during the cold work compression test. Figure 8 shows the results of an experiment measuring the effects of displacement on force at steady state, while Figure 9 displays the results of a comparison between the

FEM simulations and the experiments conducted under different CFC and TSF. Given the current arbitrary Lagrangian–Eulerian (ALE) configuration, the FEM was used to correct the mesh for extraneous distortions. When comparing the FEM findings to the experimental data, the friction experienced by each sample lubricant varies at different die strokes, with values ranging from $m = 0.33/\mu = 0.139$ and $m = 0.6/\mu = 0.215$. In comparison to the other benchmark sample, CMFO and NA-O has much higher friction in the first stages I and (ii) ($m = 0.6; \mu = 0.215$) than CMFO ($m = 0.5/\mu = 0.1875$) respectively. Nevertheless, when $m = 0.42$ or $\mu = 0.1675$, both sample tests show a substantially similar pattern to that of CFC and TSF throughout the remaining phases up to the final product. At stage I, when the CFC and TSF are $m = 0.5/\mu = 0.1875$, the friction for PKO and PMO follows the same trend, and from stage (ii) forward, the load is probably sheared at $m = 0.39/\mu = 0.159$ for both sample lubricants, until completely deformed. In contrast, PS has the smallest measured load value, and its best-fitting value, according to the finite element method, is at $m = 0.5/\mu = 0.1875$, with the trend for the remainder of the stage being best fitted at $m = 0.33/\mu = 0.139$.

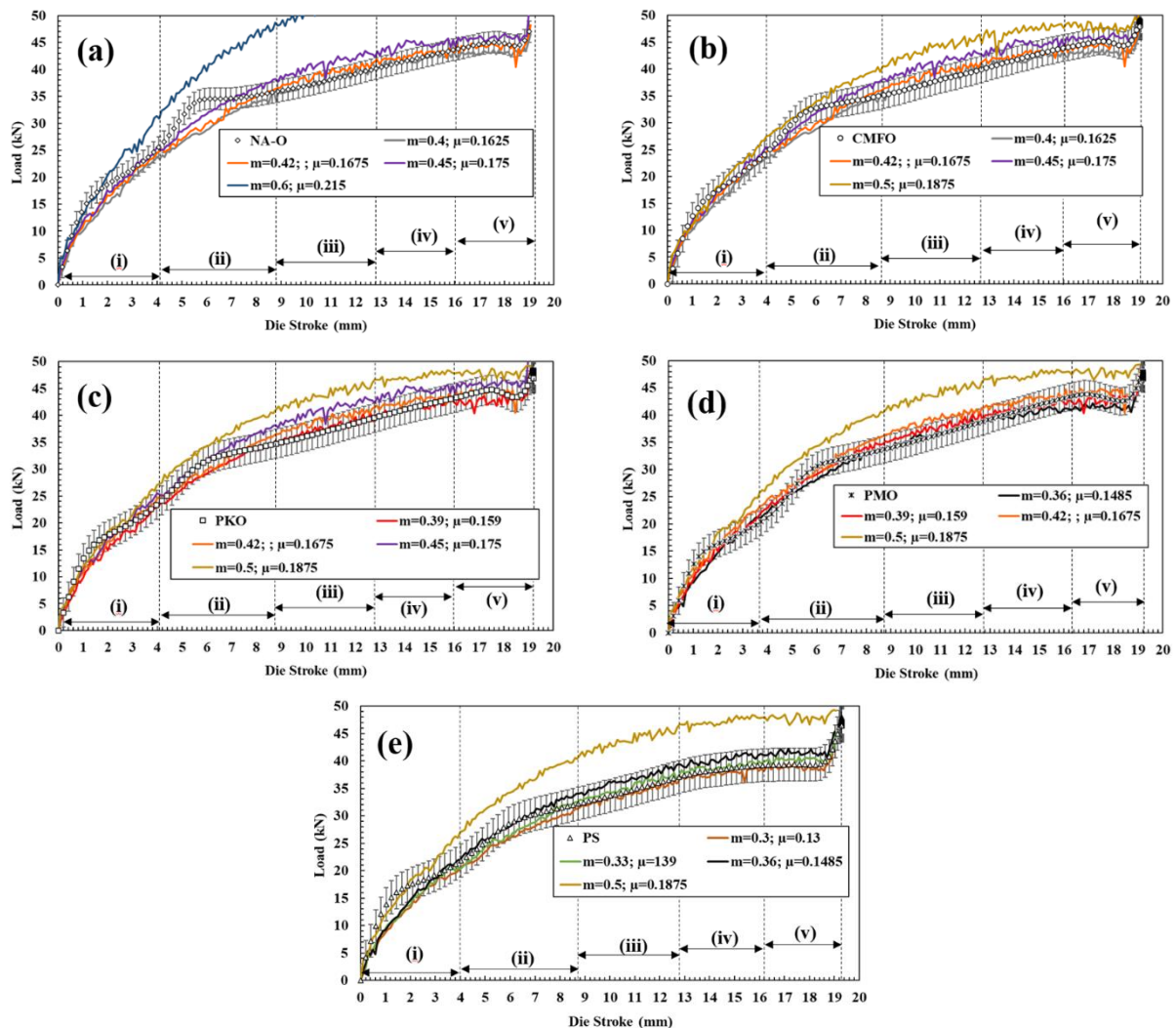


Figure 9. Verification of shear friction coefficient at varying die stroke levels for (a) NA-O, (b) CMFO, (c) PKO, (d) PMO and (e) PS [15].

After going through the process of optimization, we have come to the conclusion that the development of friction during a closed forging test may be summed up as shown in Figure 10. It appears that the friction behaves differently depending on the die stroke that is being compressed, which is in contrast to the ring compression test, in which the friction may be easily described as a single friction behavior. According to the data, PS had the least

amount of friction during the cold forging test when compared to PKO, PMO, and CMFO. PS exhibited a decreasing trend from 10% to 40% as the die stroke compression increased, and this tendency persisted until the compression was complete. Unlike PS, PMO and PKO have a slightly different tendency, in which the friction increases when the compression reaches between 40% and 50%. Another prospective palm oil-based lubricant that may be used as a metal-forming lubricant is called PMO where in comparison to CMFO, the total friction that occurs during the compression test is somewhat lower. PKO, on the other hand, demonstrates practically the same performance as CMFO in terms of friction, which tops the list when compared to other lubricants made from palm oil.

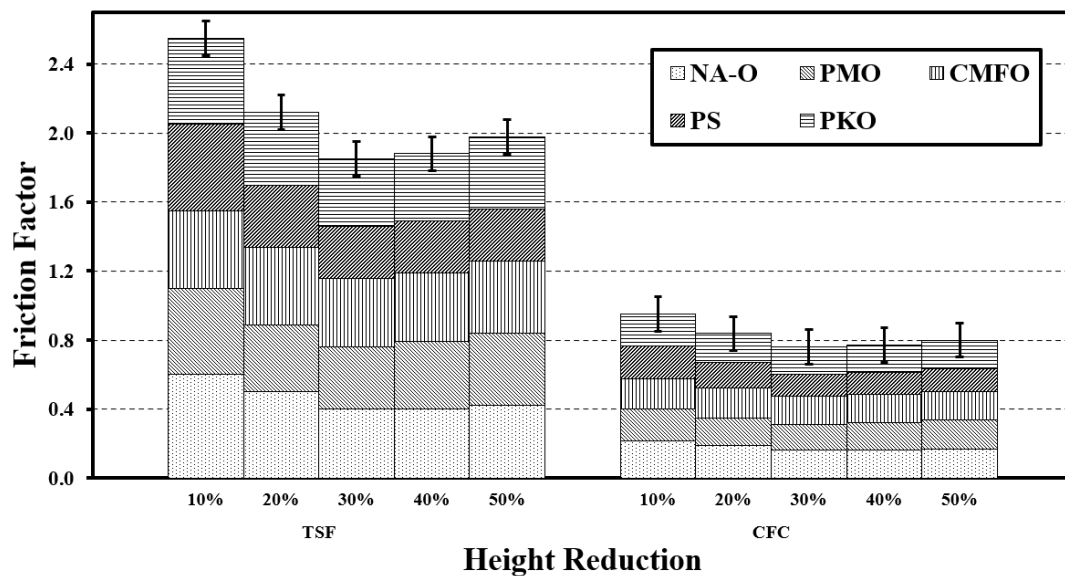


Figure 10. Summary of friction behavior for each component of the sample test following FEM optimization.

It is possible that the fatty acid chain in palm oil, which is used as a metal-forming lubricant, is responsible for its excellent performance. This chain is able to reduce the contact impact between the workpiece and the packed alkyl chain, which reacts with the cumulative short range of van der Waals forces that exist between neighboring groups [27]. A greater amount of closed-packed material led to improved affinity on the metal surface where the unsaturated fatty acid has a double bond on its ninth and tenth carbon chain, which separates it from saturated fatty acids. It was proven by Campen et al. [28] that this double bond was responsible for the formation of cis-configuration in the unsaturated oleic acid, which bent the molecules and made it difficult for them to adopt a linear molecular structure. Because of this, the unsaturated fatty acid is advantageously less efficient in the formation of close-packed monolayer soap film where a lower closed-packed density causes fatty acid chain molecules to have a lower affinity for the surfaces of metals. Meanwhile, the molecules of palmitic and stearic acid, which are saturated fatty acids, have a great capacity to pack tightly and effectively on metal surfaces [34,35].

PS PMO and PKO with high contents of saturated fatty acids displayed effective molecular packing, which protected the metal surface and suggested a reduced friction coefficient [36]. According to Zulhanafi et al. [36], a higher degree of unsaturated fatty acid lowers the capacity of the molecules to be chemisorbed; as a consequence, the metal surfaces in the fourball test experience less protection. However, during the metal-forming process, the lowest level of unsaturated fatty acid, which is PKO (17.7%), has less effect on lowering friction, when compared to PS (46.40%) and PMO (39.29%). This may be the result of very high compression on the surfaces, which reduces the strength of the intermolecular bonds and destroys the thin layer of soap film, resulting in higher friction.

4. Conclusions

In this study, commercial finite element software (DEFORM-3D) was used to simulate two forging processes of aluminum (AA1100) using different compounds of palm oil as a bio-lubricant that has been matched to CMFO. The goals of this study were to analyze the behavior of the flow of material and to predict the forging load and the stress–strain distribution during the forging process.

The results of the open and closed forging tests were shown to have significantly different patterns of frictional behavior. The interpretation of friction in open forging tests is acting as a single friction for each sample test. On the other hand, the behavior of friction in closed forging tests is different at each die stroke, and the friction varies depending on how the stroke is changed.

Both of the findings from the tribological performance of palm oil-based lubricants as metal-forming lubricants demonstrate that palm oil-based lubricants exhibit a superior performance when compared to CMFO. PS has the lowest friction for both tests where the friction in open forging is estimated at $m = 0.10/\mu = 0.05$ and in closed forging process the average is estimated at $m = 0.352/\mu = 0.17$. In open forging test also, PS shows the highest efficiency, which decreased the friction by around 77.8%, while the improvement for the PMO was approximately 66.7%. PKO, on the other hand, demonstrates a worse performance in comparison to PS and PMO, which is somewhere about 55.6%.

In light of the results of this research, one intriguing method for subsequent experiments is the modification of the lubricant, such as employing nano-lubricants in palm oil. This is because the lubrication performance requires the inclusion of additives in order to reduce the friction and improve surface protection.

Author Contributions: The idea was created by A.Y. and S.S., A.Y. was the one who came up with the hypothesis and carried out the calculations. S.S., U.A. and M.K.A.H. checked the validity of the analytical procedures. The manuscript was written by A.Y., who had assistance from U.A. and M.K.A.H. Every contributor contributed insightful comments and suggestions, which were used to improve the study, the analysis, and the manuscript. All authors have read and agreed to the published version of the manuscript.

Funding: This research received no external funding.

Data Availability Statement: There is no data availability.

Acknowledgments: The authors would like to express their thanks to the Ministry of Higher Education of Malaysia for the Konsortium Kecemerlangan Penyelidikan 2021 Research Grant (4L961) and Universiti Teknologi Malaysia (UTM) for the UTM Fundamental Research Grant (22H46).

Conflicts of Interest: The authors declare no conflict of interest.

References

1. Hassan, M.; Ani, F.N.; Syahrullail, S. Tribological performance of refined, bleached and deodorised palm olein blends bio-lubricants. *J. Oil Palm Res.* **2016**, *28*, 510–519. [[CrossRef](#)]
2. Yahaya, A.; Samion, S.; Ahyan, N.A.M.; Hamid, M.K.A. Cold extrusion using biodegradable oil as lubricant: Experimental and simulation analysis. *J. Tribol.* **2021**, *30*, 116–132.
3. Quinchia, L.A.; Delgado, M.A.; Franco, J.M.; Spikes, H.A.; Gallegos, C. Low-temperature flow behaviour of vegetable oil-based lubricants. *Ind. Crops Prod.* **2012**, *37*, 383–388. [[CrossRef](#)]
4. Syahrullail, S.; Kamitani, S.; Nakanishi, K. Experimental evaluation of refined, bleached, and deodorized palm olein and palm stearin in cold extrusion of aluminum A1050. *Tribol. Trans.* **2012**, *55*, 199–209. [[CrossRef](#)]
5. Golshokouh, I.; Syahrullail, S.; Ani, F.N.; Masjuki, H.H. Investigation of palm fatty acid distillate as an alternative lubricant of petrochemical based lubricants, tested at various speeds. *Int. Rev. Mech. Eng.* **2013**, *7*, 72–80.
6. Zulhanafi, P.; Syahrullail, S.; Ahmad, M.A. The tribological performance of hydrodynamic journal bearing using bio-based lubricant. *Tribol. Ind.* **2020**, *42*, 278. [[CrossRef](#)]
7. Kramer, P.; Groche, P. Friction measurement under consideration of contact conditions and type of lubricant in bulk metal forming. *Lubricants* **2019**, *7*, 12. [[CrossRef](#)]

8. Okokpujie, I.P.; Tartibu, L.K.; Sinebe, J.E.; Adeoye, A.O.; Akinlabi, E.T. Comparative Study of Rheological Effects of Vegetable Oil-Lubricant, TiO₂, MWCNTs Nano-Lubricants, and Machining Parameters' Influence on Cutting Force for Sustainable Metal Cutting Process. *Lubricants* **2022**, *10*, 54. [[CrossRef](#)]
9. Moshkovich, A.; Perfilyev, V.; Rapoport, L. Effect of plastic deformation and damage development during friction of FCC metals in the conditions of boundary lubrication. *Lubricants* **2019**, *7*, 45. [[CrossRef](#)]
10. Hafis, S.M.; Ridzuan, M.J.M.; Farahana, R.N.; Ayob, A.; Syahrullail, S. Paraffinic mineral oil lubrication for cold forward extrusion: Effect of lubricant quantity and friction. *Tribol. Int.* **2013**, *60*, 111–115. [[CrossRef](#)]
11. Groche, P.; Kramer, P.; Bay, N.; Christiansen, P.; Dubar, L.; Hayakawa, K.; Hu, C.; Kitamura, K.; Moreau, P. Friction coefficients in cold forging: A global perspective. *CIRP Ann.* **2018**, *67*, 261–264. [[CrossRef](#)]
12. Zhang, D.W.; Ou, H. Relationship between friction parameters in a Coulomb–Tresca friction model for bulk metal forming. *Tribol. Int.* **2016**, *95*, 13–18. [[CrossRef](#)]
13. Du, F.; Li, C.; Li, D.; Sa, X.; Yu, Y.; Li, C.; Yang, Y.; Wang, J. Research Progress Regarding the Use of Metal and Metal Oxide Nanoparticles as Lubricant Additives. *Lubricants* **2022**, *10*, 196. [[CrossRef](#)]
14. Sani, A.; Sahab, A.; Abd Rahim, E.; Talib, N.; Kamdani, K.; Rahim, M.Z. Performance Evaluation of Palm-Olein TMP Ester Containing Hexagonal Boron Nitride and an Oil Miscible Ionic Liquid as Bio-Based Metalworking Fluids. *J. Mech. Eng.* **2017**, *4*, 223–234.
15. Aiman, Y.; Syahrullail, S.; Hamid, M.K.A. Optimisation of friction surfacing process parameters for a1100 aluminium utilising different derivatives of palm oil based on closed forging test. *Biomass Convers. Biorefin.* **2022**, 1–18. [[CrossRef](#)]
16. Stoffel, W.; Chu, F.; Ahrens, E.H. Analysis of long-chain fatty acids by gas-liquid chromatography. *Anal. Chem.* **1959**, *31*, 307–308. [[CrossRef](#)]
17. Aiman, Y.; Syahrullail, S. Frictional and material deformation of aluminium alloy in cold forging test under different derivatives of palm oil lubrication condition. *J. Braz. Soc. Mech. Sci. Eng.* **2022**, *44*, 396. [[CrossRef](#)]
18. Abdulmawlla, M.A. Finite Element Analysis and Optimization of Closed Die Forging Process for Aluminium Metal Matrix Composites. Ph.D. Thesis, Universiti Putra Malaysia, Serdang, Malaysia, 2010.
19. Okokpujie, I.P.; Chima, P.C.; Tartibu, L.K. Experimental and 3D-Deform Finite Element Analysis on Tool Wear during Turning of Al-Si-Mg Alloy. *Lubricants* **2022**, *10*, 341. [[CrossRef](#)]
20. Li, F.; Chen, P.; Han, J.; Deng, L.; Yi, J.; Liu, Y.; Eckert, J. Metal flow behavior of P/M connecting rod preform in flashless forging based on isothermal compression and numerical simulation. *J. Mater. Res. Technol.* **2020**, *9*, 1200–1209. [[CrossRef](#)]
21. Patwardhan, P.S.; Nalavde, R.A.; Kujawski, D. Estimation of Ramberg-Osgood Constants for Materials with and without Luder's Strain Using Yield and Ultimate Strengths. *Procedia Struct. Integr.* **2019**, *17*, 750–757. [[CrossRef](#)]
22. Szala, M.; Winiarski, G.; Wójcik, L.; Bulzak, T. Effect of Annealing Time and Temperature Parameters on the Microstructure, Hardness, and Strain-Hardening Coefficients of 42CrMo4 Steel. *Materials* **2020**, *13*, 2022. [[CrossRef](#)]
23. Tiong, C.I.; Azli, Y.; Kadir, M.R.A.; Syahrullail, S. Tribological evaluation of refined, bleached and deodorized palm stearin using four-ball tribotester with different normal loads. *J. Zhejiang Univ. Sci. A* **2012**, *13*, 633–640. [[CrossRef](#)]
24. Wang, J.P. A new evaluation to friction analysis for the ring test. *Int. J. Mach. Tools Manuf.* **2001**, *41*, 311–324. [[CrossRef](#)]
25. Farhanah, A.N.; Syahrullail, S.; Ajruddin, M.A. Evaluation of RBD palm stearin as alternative lubricant for cold forward extrusion process. *J. Phys. Conf. Ser.* **2017**, *908*, 012062. [[CrossRef](#)]
26. Maleque, M.A.; Masjuki, H.H.; Sapuan, S.M. Vegetable-based biodegradable lubricating oil additives. *Ind. Lubr. Tribol.* **2003**, *55*, 137–143. [[CrossRef](#)]
27. Crespo, A.; Morgado, N.; Mazuyer, D.; Cayer-Barrioz, J. Effect of Unsaturation on the Adsorption and the Mechanical Behavior of Fatty Acid Layers. *Langmuir* **2018**, *34*, 4560–4567. [[CrossRef](#)]
28. Campen, S.; Green, J.H.; Lamb, G.D.; Spikes, H.A. In situ study of model organic friction modifiers using liquid cell AFM; saturated and mono-unsaturated carboxylic acids. *Tribol. Lett.* **2015**, *57*, 18. [[CrossRef](#)]
29. Zhang, D.W.; Cui, M.C.; Cao, M.; Ben, N.Y.; Zhao, S.D. Determination of friction conditions in cold-rolling process of shaft part by using incremental ring compression test. *Int. J. Adv. Manuf. Technol.* **2017**, *91*, 3823–3831. [[CrossRef](#)]
30. Caminaga, C.; da Silva Issii, R.L.; Button, S.T. Alternative lubrication and lubricants for the cold extrusion of steel parts. *J. Mater. Process. Technol.* **2006**, *179*, 87–91. [[CrossRef](#)]
31. Nurul, M.A.; Syahrullail, S. Lubricant viscosity: Evaluation between existing and alternative lubricant in metal forming process. *Procedia Manuf.* **2015**, *2*, 470–475. [[CrossRef](#)]
32. Yingying, L.; Houfang, L.; We, J.; Dongsheng, L.; Shijie, L.; Bin, L. Biodiesel Production from crude *Jatropha curcas* L. Oil with Trace Acid Catalyst. *Chin. J. Chem. Eng.* **2012**, *20*, 740–746.
33. Liu, Y.; Lu, H.; Jiang, W.; Li, S.; Liu, S.; Liang, B. Biodiesel production from crude *Jatropha curcas* L. oil with trace acid catalyst. *Chin. J. Chem. Eng.* **2012**, *20*, 740–746. [[CrossRef](#)]
34. Razak, D.M.; Syahrullail, S.; Sapawe, N.; Azli, Y.; Nuraliza, N. A new approach using palm olein, palm kernel oil, and palm fatty acid distillate as alternative biolubricants: Improving tribology in metal-on-metal contact. *Tribol. Trans.* **2015**, *58*, 511–517. [[CrossRef](#)]

35. Wood, M.H.; Casford, M.T.; Steitz, R.; Zarbakhsh, A.; Welbourn, R.J.L.; Clarke, S.M. Comparative adsorption of saturated and unsaturated fatty acids at the iron oxide/oil interface. *Langmuir* **2016**, *32*, 534–540. [[CrossRef](#)]
36. Zulhanafi, P.; Syahrullail, S. The tribological performances of Super Olein as fluid lubricant using four-ball tribotester. *Tribol. Int.* **2019**, *130*, 85–93. [[CrossRef](#)]

Disclaimer/Publisher's Note: The statements, opinions and data contained in all publications are solely those of the individual author(s) and contributor(s) and not of MDPI and/or the editor(s). MDPI and/or the editor(s) disclaim responsibility for any injury to people or property resulting from any ideas, methods, instructions or products referred to in the content.